A Virtual Manipulator Model for Space Robotic Systems

S. Dubowsky and Z. Vafa
Massachusetts Institute of Technology
Cambridge, MA 02139

1. Abstract

Future robotic manipulators carried by a spacecraft will be required to perform complex tasks in space, like repairing satellites. Such applications of robotic manipulators will encounter a number of kinematic, dynamic and control problems due to the dynamic coupling between the manipulators and the spacecraft. This paper presents a new analytical modeling method for studying the kinematics and dynamics of manipulators in space. The problem is treated by introducing the concept of a Virtual Manipulator (VM). The kinematic and dynamic motions of the manipulator, vehicle and payload, can be described relatively easily in terms of the Virtual Manipulator movements, which have a fixed base in inertial space at a point called a Virtual Ground. It is anticipated that the approach described in this paper will aid in the design and development of future space manipulator systems.

2. Introduction

Robotic manipulators are potentially very useful for performing complex tasks in non-industrial hostile environments [1,2], such as in space. A number of studies have considered the potential applications of manipulators in space and the capabilities that these systems must have to achieve anticipated mission goals [3-5]. These applications include tasks such as repairing, servicing and constructing space stations in orbit. Currently, these tasks can only be performed by astronaut Extra Vehicular Activity (EVA). Eliminating the need for EVA would obviously reduce hazards to the astronauts and mission costs.

Unfortunately, the use of manipulators in space is complicated by the manipulator/spacecraft dynamic coupling. For example, movements of a manipulator will disturb the attitude of the spacecraft carrying it. This coupling will adversely affect the manipulator's precision, and reduce the on orbit life of the system by consuming excessive attitude control fuel. Also, any motions of the spacecraft, say due to the firing of attitute control jets, will disturb the manipulator. Therefore, new manipulator concepts, designs and control techniques will be required to minimize and compensate for the manipulator/spacecraft dynamic coupling.

Researchers working on the control of space manipulators have focused their attention on issues such as sensor reqirements, path planning algorithms, teleoperator control [6-8]; the problems of vehicle/manipulator dynamic interactions remain unresolved.

This paper presents a new and effective analytical modeling method for studying the kinematics and dynamics of manipulators in space. The problem is treated by introducing the concepts of a Virtual Ground (VG) and Virtual Manipulator (VM). As discussed below the VG is located at the center of mass of the manipulator/spacecraft system, and the VM is an ideal kinematic chain connecting the VG to any point on the real manipulator. Motions of a system, including a vehicle, manipulator and payload can be described easily by the VM. This model has proven to be effective in calculating the kinematic and dynamic properties of the system; such as its inverse kinematic solution and workspaces. This paper shows that the VM approach can also be used to plan the manipulator's motions in order to minimize the degrading consequences of the manipulator/spacecraft dynamic interactions.

3. A Model of Manipulators in Space

Future space manipulator systems will have one or more mechanical arms carried by a vehicle, as shown in Figure 1. The vehicle will be capable of motion in six degrees of freedom, and will have reaction jets for position and attitude control. Although manipulators could be driven by photovoltaicly powered electric actuators, which use no

where

$$M_{tot} = \sum_{q=1}^{N} M_q \tag{2}$$

Since there are no external forces, the VG is stationary in the frame N and the vector $\mathbf{V}_g$ is always constant.

In the following development the VM properties such as link dimensions and joint axes, for initial manipulator configuration are described. Then the rules for its joint movements as a function of the real manipulator joint movements are presented. Referring to Figure 3, which shows the end effector VM for the manipulator shown in Figure 2, the i^{th} link of the Virtual Manipulator is defined by the vector $\mathbf{V}_i$,

$$\begin{aligned} \mathbf{V}_1 &= \mathbf{D}_1 \\ \mathbf{V}_2 &= \mathbf{H}_1 + \mathbf{D}_2 \\ &\vdots \\ \mathbf{V}_N &= \mathbf{H}_{N-1} + \mathbf{D}_N \end{aligned} \tag{3}$$

where

$$\mathbf{D}_i = \mathbf{R}_i \sum_{q=1}^{i} M_q / M_{tot} \qquad (i = 1, 2, ..., N) \tag{4}$$

and

$$\mathbf{H}_i = \mathbf{L}_i \sum_{q=1}^{i} M_q / M_{tot} \qquad (i = 1, 2, ..., N-1) \tag{5}$$

The first VM link represents the vehicle's orientation. This link is attached to the VG by a spherical joint and its motion is equal to the three vehicle rotations with respect to inertial space. The end of the Virtual Manipulator terminates at the end effector, defined by a vector $\mathbf{E}$, fixed in the N^{th} VM link.

The i^{th} VM joint is taken as a revolute or a prismatic joint depending upon whether the i^{th} joint of the real manipulator is revolute or prismatic. The axis of rotation for a revolute VM joint, j_i, is parallel to the axis of the real manipulator joint A_i. Similarly, the translational axes of prismatic VM joints are parallel to the corresponding axes of the real manipulator prismatic joints. Equations (1) through (5) define the VM and its position corresponding to the initial position of the system, as shown in Figure 2. The VM links will all be parallel to the real manipulator links in cases where all the centers of mass for all manipulator links lie on a line connecting the manipulator joints on the corresponding link.

The VM will move as the joints of the real manipulator move. The angular rotations of the VM revolute joints, from their initial position, are equal to the angular rotations of the corresponding revolute joints for the real manipulator. The prismatic virtual joint translations are ratios of the corresponding real prismatic joint translations. For an end effector VM, translation of the virtual joint, $\mathbf{P}_j$, is given by:

$$\mathbf{P}_j = \mathbf{T}_j \sum_{q=1}^{j} M_q / M_{tot} \tag{6}$$

For the VM in its position of construction, its initial position, the values of $\mathbf{T}_j$ are taken as zero. Hence the initial magnitudes of $\mathbf{P}_j$ are zero. The prismatic joint motions, $\mathbf{T}_j$, are referenced to the initial position.

If a VM that is constructed according to Equations (1) through (5), moves with the real manipulator according to the above description, and its link shapes and lengths remain constant as the manipulator moves, then it can be shown (see Appendix A) that:

1 The axis of the i^{th} virtual joint is always parallel to the i^{th} axis of the real system joint, and

2 The Virtual Manipulator end point will always coincide with the real manipulator's end effector.

These properties enable the kinematic and dynamic motions of a free-floating manipulator system to be described by the motions of a much simpler Virtual Manipulator which has a fixed base in inertial space. The properties of the VM remain the same as long as the mass property of the system does not change. For example, when the manipulator grasps a free-floating pay load, the VM changes. According to Equations (1) through (5), the VM link lengths will be reduced for the addition of a payload. Virtual Manipulators constructed for points other than the end effector have different links than the links defined in Equation (1); and their joint movements maybe different than the ones described above, for example, prismatic joint translations may be the vector $(\mathbf{P}_i - \mathbf{T}_i)$, depending upon location of the point used to construct the VM [9].

reaction fuel, manipulator motions could disturb a vehicle's position and attitude and result in the consumption of excessive amounts of attitude fuel. The useful life of spacecraft systems is often limited by the amount of reaction jet fuel they can carry.

Two approaches to solve this problem are: 1) permit the vehicle to move and compensate for the base motions in the manipulator task planning; and 2) plan the manipulator motions so that they do not cause the vehicle to move excessively. The first of these approaches requires the ability to perform inverse kinematic and workspace calculations for a free-floating system [10]. The second requires methods for planning manipulator motions that would self-correct the vehicle's orientation with little or no reaction jet adjustments. These approaches and associated issues are addressed here through the Virtual Manipulator technique. Assumed in this work is that the external forces/torques acting on the system are negligible, and that the system is free floating. Also assumed is that the system elements may be modeled as rigid bodies. The later assumption may not be valid if a manipulator must perform high speed motions.

4. Analytical Development of the Virtual Manipulator

The Virtual Manipulator (VM) is a massless kinematic chain terminating at an arbitrary point on the real manipulator. Its base is the Virtual Ground (VG), which is an imaginary fixed point in inertial space. It is proven below that for a given system the properties of the VM and location of the VG are fixed. VMs exist for many different manipulator structures, such as open or closed chains, single or many branch arms, revolute or prismatic joints [9-11]. The discussion in this paper will be limited to manipulators composed of spatial serial chains with revolute or prismatic connections. Although VMs exist for any point on the real manipulator, this paper deals with VMs whose end points coincide with the real manipulator end effector.

The VG is defined to be the center of mass of the manipulator system. From elementry mechanics, when there are no external forces, such as from reaction jets, the VG will be fixed in an inertial space. It will not move due to any internal forces of the system such as joint torques, or due to any manipulator motions.

Figure 2 shows a schematic drawing of an N body spatial manipulator system. The first body in the chain represents the vehicle which carries the manipulator. The N^{th} body is a combination of the payload and the last link. The i^{th} joint is called J_i, and C_i is the center of mass of the i^{th} body. The vectors $\mathbf{R}_i$ and $\mathbf{L}_i$ connect C_i to J_i and J_i to C_{i+1}, respectively. The vector $\mathbf{R}_N$ connects C_N to the end effector. The vectors $\mathbf{R}_i$ and $\mathbf{L}_{i-1}$ are fixed relative to the i^{th} link, and hence the angle between these vectors is constant for all system configurations. If the i^{th} manipulator joint is a revolute joint, the vector defining the axis of rotation of J_i is called $\mathbf{A}_i$, and the angle θ_i is the rotation of the i^{th} joint. If the i^{th} manipulator joint is a prismatic joint, the vector $\mathbf{T}_i$ is defined to be the translation along the translational axis. If the i^{th} joint is revolute, then the magnitude T_i is equal to zero.

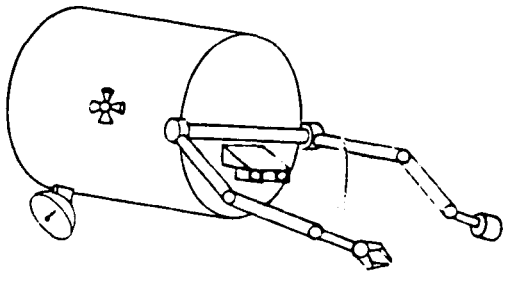

Figure 1: A Space Manipulator System.

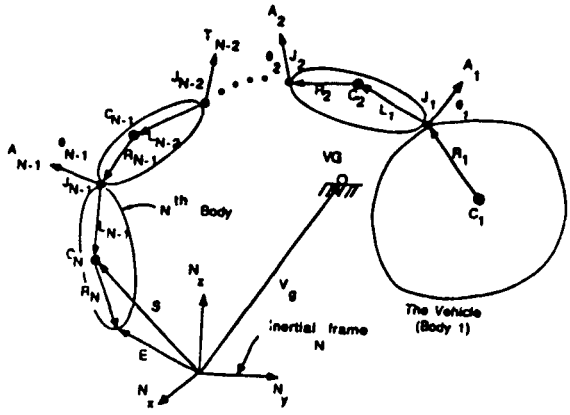

Figure 2: N Body System in Space.

The location of the VG for this system in inertial space, the center of mass of the system, can be found by knowing some initial position of the system. The vector S(0) defines the initial known location of the end effector with respect to an inertial reference frame N. Then the location of the VG, the vector $\mathbf{V}_g$, can be obtained from conservation of linear momentum by:

$$\mathbf{V}_g = \sum_{i=1}^{N}[\mathbf{S}(0) - \sum_{j=1}^{i-1}(\mathbf{R}_j + \mathbf{L}_j + \mathbf{T}_j)]M_i/M_{tot} \qquad (1)$$

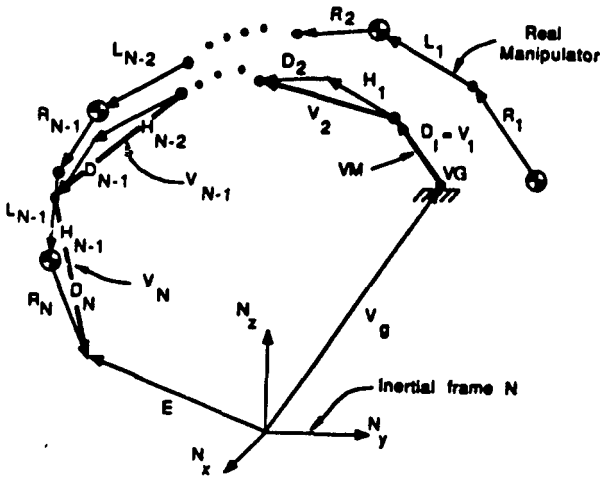

Figure 3: N Body System and its VM.

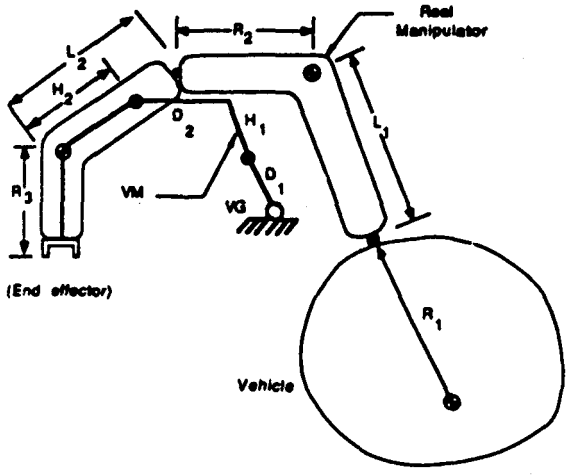

Figure 4: A Three Body Planar System and its VM.

Table 1 gives the properties of a very simple planar manipulator and its Virtual Manipulator, shown in Figure 4. It should be remembered that the method is not restricted to planar systems.

5. Applications of Virtual Manipulators

The Virtual Manipulator approach has a number of possible applications. VMs can be used to simplify the inverse kinematics of space manipulators, calculate their workspaces, plan their motions and formulate the equations of motion [9-11]. It should be noted that using conventional methods, these problems are far more difficult for space manipulators than for industrial manipulators with fixed bases. In the sections below, the use of the VM is shown for workspace analysis and path planning.

A. Workspace Analysis

Since the vehicle and manipulator dynamics are coupled, the manipulator's motions will cause the vehicle to move and this in turn makes it difficult to find the manipulator workspace. In fact several different types of workspaces exist. In this section, a workspace called the constrained workspace, for a manipulator in space is defined, for a more complete discussion of space manipulator workspaces refer to references [9,10]. For the constrained workspace it is assumed that the attitude, but not the location, of the vehicle is controlled. This can be achieved without the use of attitude control fuel by employing reaction wheels, or by using the self correcting maneuvers discussed later in this paper.

To find the constrained workspace, a Virtual Manipulator is constructed to the end effector of the real manipulator. The joint limits of the real manipulator are transformed into VM joint limits. The workspace of the Virtual Manipulator is then found using conventional workspace analysis methods [12]. The real manipulator workspace will be equal to the VM workspace because of the following reasons. The VM end point coincides with the real manipulator end effector, and it is assumed that it is possible to control the orientation of the first VM link, representing the vehicle, with respect to inertial space. The other joints are controlled with their actuators. This workspace will always be a spherical shell, assuming there are no limits on the vehicle orientations. Figure 5 shows the constrained workspace for the simple two link manipulator shown in Figure 4, it was found using its VM.

B. Path Planning

In certain cases, the magnitude of the rotations of the vehicle caused by the manipulator's motion may not be acceptable. For example, vehicle rotations may cause communication devices to loose their signals. Vehicle rotations can be controlled using reaction wheels or reaction jets. However, these devices have the disadvantages of increased mechanical complexity and system weight or increased consumption of attitude control fuel.

It is shown below that the manipulator itself can be moved in such a way as to have the end effector follow a nominal specified path and yet have a prescribed vehicle orientation, with specified limits, without using attitude control fuel or requiring reaction wheels.

Table 1: Characteristics of Planar Manipulator and its VM.

Body no	M (Kg)	R (m)	L (m)	D (m)	H (m)
1	50	1.0	1.0	0.33	0.33
2	50	0.75	0.75	0.5	0.5
3	50	0.5	-	0.5	-

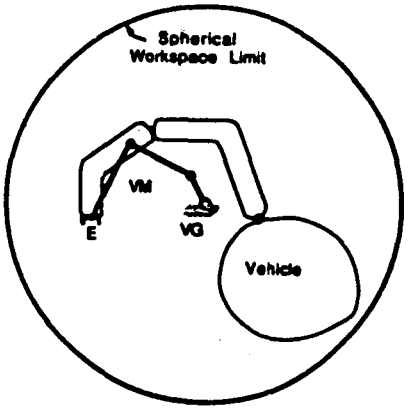

Figure 5: Constrained Workspace of Manipulator Shown in Figure 4.

To find this motion the principle of conservation of angular momentum is applied to the system. For an n degrees of freedom space manipulator the following equation can be written.

$$\dot{\mathbf{X}} = \mathbf{F}(\Theta, \mathbf{X})\dot{\Theta}, \tag{7}$$

$\mathbf{F}$: 3 by n matrix with elements $F_{i,j}$,

$\mathbf{X}$: 3 by 1 vector of vehicle inertial orientations with elements, X_i,

Θ : n by 1 vector of joint angles with elements θ_i

In general, Equation (7) is non-integratable, that is:

$$\frac{\partial^2 X_i}{\partial \theta_k \partial \theta_j} \neq \frac{\partial^2 X_i}{\partial \theta_j \partial \theta_k} \tag{8}$$

Therefore, the final vehicle orientation depends on path taken by the manipulator from one position to another. It follows that the final vehicle orientation will change if the manipulator moves along one path in joint space and returns to its initial position by another path. This is a similar notion to the one which permits astronauts to reorient their bodies by moving their limbs [13]. This leads to a strategy for adjusting or correcting motions of the vehicle's orientation. In this strategy nominal trajectories are selected for the end effector and vehicle orientation. Then the joint motions are executed assuming the vehicle follows its trajectory. If at any point the vehicle orientation deviates from its desired path by more than a specific amount, a series of small cyclic motions, selected to correct for the vehicle orientation are added to the joint motions.

To find the cyclical joint motions that achieve the desired vehicle/base orientation corrections, it is assumed that these motions are small enough that the end effector deviates only by a small amount from its nominal trajectory. This small motion assumption permits the use of a nonlinear system model in which nonlinearities of order greater than 2 can be neglected.

First, let $\mathbf{X}$ be a set of Euler angles defining the base orientation with respect to an inertial coordinate frame. The initial and desired final base orientations are $\mathbf{X}_i$ and $\mathbf{X}_d$, respectively. The desired change in the Euler angles is defined by

$$\delta\mathbf{X} = \mathbf{X}_i - \mathbf{X}_d \tag{9}$$

Let Θ_0 be the vector defining the initial and final joint positions at the beginning and end of the correction maneuver. Also let the vectors $\delta\mathbf{V}$ and $\delta\mathbf{W}$ define small joint movements. The closed correction path is constructed by having the manipulator move along the straight lines, in joint space defined by vectors $\delta\mathbf{V}$ and $\delta\mathbf{W}$ shown in Figure 6.

For small $\delta\mathbf{V}$ and $\delta\mathbf{W}$ the following equation can be obtained from Equation (7).

$$\delta X_k = \sum_{i=1}^{3}\sum_{j=1}^{3}\left[\sum_{m=1}^{3}\left(\frac{\partial F_{kj}}{\partial X_m}F_{mi} - \frac{\partial F_{ki}}{\partial X_m}F_{mj}\right) + \frac{\partial F_{kj}}{\partial \theta_i} - \frac{\partial F_{ki}}{\partial \theta_j}\right]\delta W_j \delta V_i \qquad (k = 1,2,3) \tag{10}$$

where δX_i, δV_i and δW_i are elements of the vectors $\delta\mathbf{X}$, $\delta\mathbf{V}$ and $\delta\mathbf{W}$, respectively. In the case of a three DOF spatial manipulator, Equation (10) will yield three equations with six unknowns. Three additional constrain equations are required to solve for $\delta\mathbf{V}$ and $\delta\mathbf{W}$.

If vectors $\delta\mathbf{V}$ and $\delta\mathbf{W}$ are parallel, the cyclic motion will not produce any vehicle rotation. Therefore it is assumed that these vectors are perpendicular:

$$\delta\mathbf{V}^T \cdot \delta\mathbf{W} = 0. \tag{11}$$

Further, the magnitudes of $\delta\mathbf{W}$ and $\delta\mathbf{V}$ are assumed to be equal:

$$\delta\mathbf{V}^T \cdot \delta\mathbf{V} = \delta\mathbf{W}^T \cdot \delta\mathbf{W}, \tag{12}$$

and one of the elements of $\delta\mathbf{V}$ is chosen to be a linear combination of the other two. For example,

$$\delta V_3 = (\delta V_2 + \delta V_1)/2 \tag{13}$$

Equations (10) through (13) yield six scalar equations with six scalar unknowns, which can be solved for the desired joint trajectories, $\delta\mathbf{V}$ and $\delta\mathbf{W}$. If the required correction, $\delta\mathbf{X}$, is large, the values of $\delta\mathbf{V}$ and $\delta\mathbf{W}$ may violate the small joint motion assumption. In this case the desired correction can be achieved by a series of m cyclical correction maneuvers. It is shown below that at each cycle Equations (10) through (13) do not have to be resolved and the final position can be achieved.

Referring to Figure 7, $\mathbf{T}(\mathbf{X}_j)$ is a 3 by 3 matrix which transforms a vector expressed in vehicle body coordinates (x,y,z) into inertial or Newtonian coordinates (N_x,N_y,N_z), when the body is at jth orientation. The transformation matrix for the initial vehicle orientation is $\mathbf{T}(\mathbf{X}_i)$. The transformation matrix for the desired vehicle position to be achieved after m cycles is $\mathbf{T}(\mathbf{X}_d)$. After one correction cycle, the transformation matrix is $\mathbf{T}(\mathbf{X}_i + \delta\mathbf{x})$, where,

$$\mathbf{T}(\mathbf{X}_i + \delta\mathbf{x}) = \mathbf{T}(\mathbf{X}_i)\mathbf{A}, \tag{14}$$

and the matrix $\mathbf{A}$ is the transformation matrix from the vehicle position, one cycle from the initial vehicle position, back to the initial position. The $\mathbf{A}$ matrix will not change with each cycle because the total system, vehicle and manipulator, have been subject only to a rigid body rotation in inertial space. Hence after m cycles the transformation matrix from the desired system position to inertial coordinates is simply:

$$\mathbf{T}(\mathbf{X}_d) = \mathbf{T}(\mathbf{X}_i)\mathbf{A}^m \tag{15}$$

Equation (15) can be solved for $\mathbf{A}$:

$$\mathbf{A} = \mathbf{P}\Lambda^{1/m}\mathbf{P}^{-1} \tag{16}$$

where Λ is a diagonal matrix of the eigenvalues of $\mathbf{T}(\mathbf{X}_i)^{-1}\mathbf{T}(\mathbf{X}_d)$ and $\mathbf{P}$ is a matrix of corresponding eigenvectors.

Using the $\mathbf{A}$ matrix obtained from Equation (16), the change in Euler angles ($\delta\mathbf{x}$) are calculated from Equation (14). Then the joint correction motions for each cycle, $\delta\mathbf{V}$, $\delta\mathbf{W}$) m times to approach the desired vehicle orientation. However, the final vehicle orientation after m cycles will usually be slightly different than the desired orientation because of the neglected higher order nonlinearities. In order to achieve the desired vehicle orientation more precisely, the over all correction may need to be broken into several smaller corrections and the process repeated with a slightly different set of $\delta\mathbf{V}$ and $\delta\mathbf{W}$ for each subcorrection.

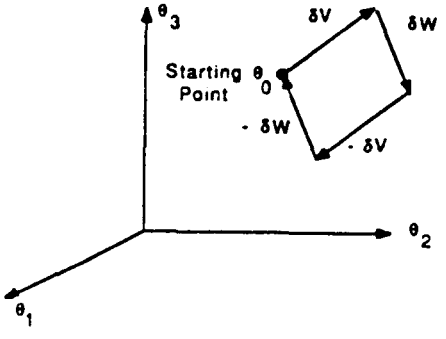

Figure 6: A Closed Path Correction in Joint Space for a Vehicle Rotation.

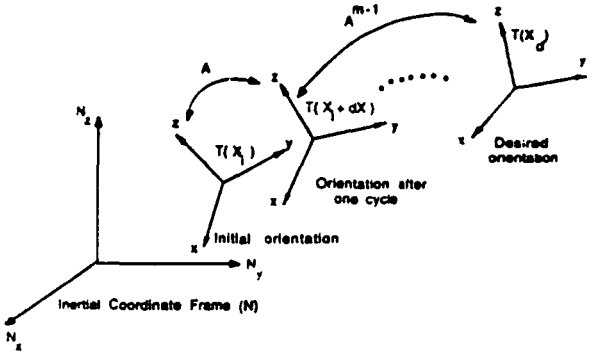

Figure 7: Vehicle Coordinate Rotation Due to Cyclic Manipulator Motion.

The above technique is now demonstrated for a spatial 3 DOF space manipulator shown in Figure 8. The properties of the manipulator are given in Table 2. It is desired to rotate the vehicle from its initial orientation to its final orientation as shown in Table 3. In this example, it was necessary to solve for the joint trajectories (δV and δW) 3 times to precisely obtain the desired vehicle orientation. The joint trajectories for these 3 cycle sets are shown in Figures 9 through 11. Each cycle is repeated 30 times to achieve the desired vehicle orientation. Table 3 shows the system angles after each cycle set. During each cycle the vehicle oscillates in sympathy to the manipulator's motion, see Figure 12. However the mean orientation of the vehicle changes continuously and reaches $\mathbf{X}_d$ at the same time the joints return to their initial positions. Figure 13 shows the mean vehicle orientation during the joint cycles. The vehicle movements during the joint motions are $\pm$ 0.1 radians from their mean trajectory. Here one can clearly see change in the base orientation as the manipulator joints cycle through their motion.

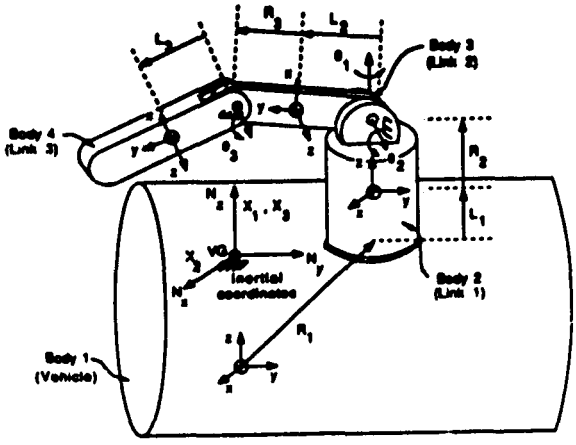

Figure 8: Spatial 3 DOF Space Manipulator.

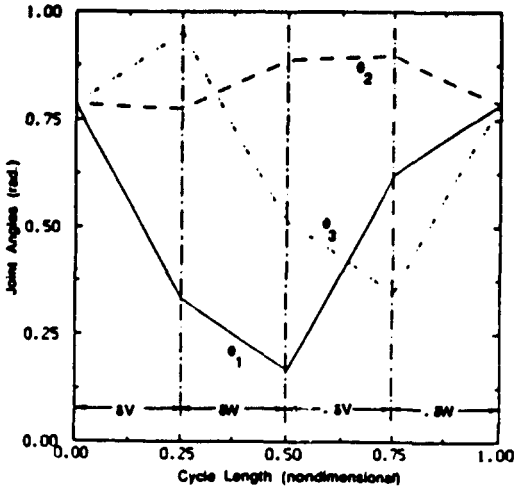

Figure 9: Joint Angle Trajectories for First Set of Cycles.

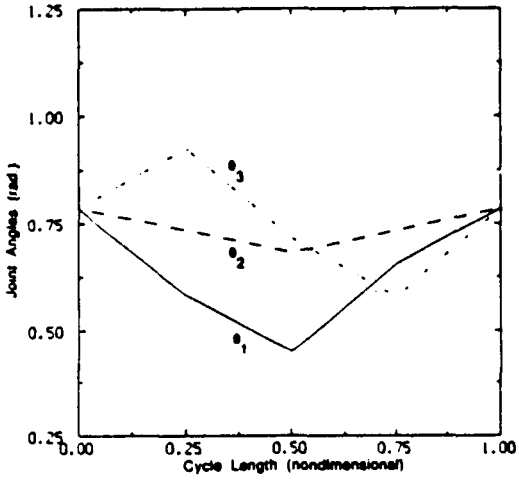

Figure 10: Joint Angle Trajectories for Second Set of Cycles.

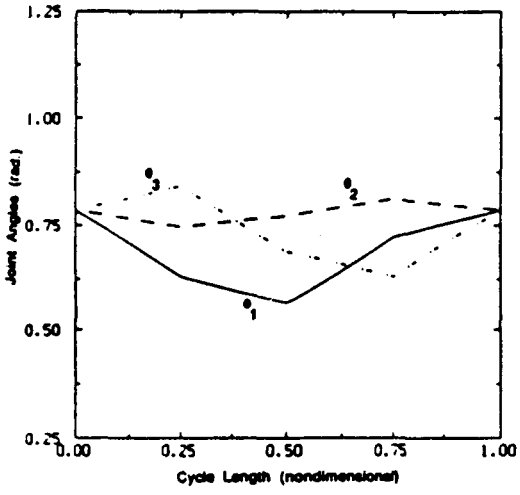

Figure 11: Joint Angle Trajectories for third Set of Cycles.

Table 3: Manipulator Angles at Different Instances.

Angles (deg)	Initial	desired	After one cycle set	After second cycle set	Final position
X_1	50.	45.	44.7	45.0	45.0
X_2	40.	45.	43.9	45.0	45.0
X_3	35.	35.	37.1	34.8	35.0
θ_1	45.	45.	45.	45.	45.0
θ_2	45	45.	45.	45.	45.0
θ_3	45.	45.	45.	45.	45.0

Table 2: Three DOF Manipulator Characteristics.

Body no.	Mass (kg)	R in local coord. (m)	L in local coord. (m)	Inertia about prin. axis (Kg-m^2)
1	20.	-1 i +1 j +2k	0.1 i + 0.5 j	0.5 i , 0.5 j , 0.5 k
2	7.	0.5 i	0.5 i	0.5 i , 0.5 j , 0.5 k
3	7.	0.5 i +0.1 k	0.5 i +0.1 k	0.5 i , 0.1 j , 0.5 k
4	5.	-	-	0.5 i , 0.1 j , 0.5 k

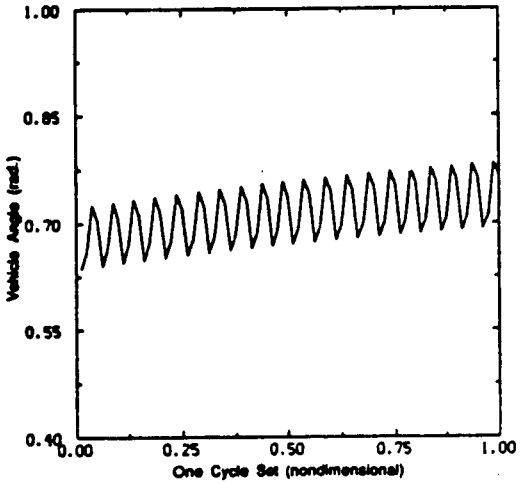

Figure 12: The X_2 Vehicle Coordinate for the First Set of Cycles.

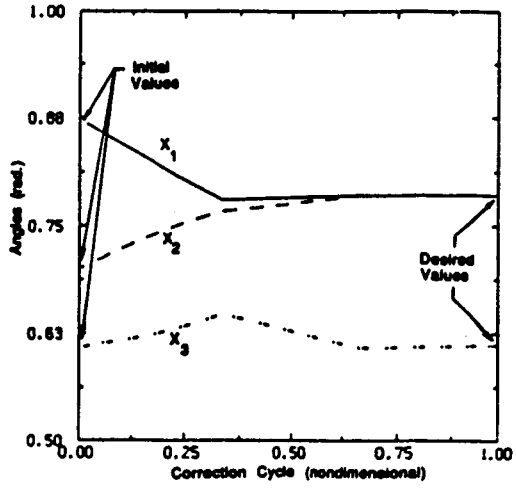

Figure 13: Mean Vehicle Euler Angles During Correction Cycle.

6. Summary and Conclusion

In this paper, the concepts of Virtual Manipulators and Virtual Grounds are discussed. The end effector VM characteristics and proof of its properties for serial link with revolute and prismatic joints were presented, and some of its applications were discussed. This is a new concept and further research is required to demonstrate its full capabilities.

7. Acknowledgement

The support of this research by the Automation Branch of NASA Langley Research Center under Grant NAG-1-489 is acknowledged.

8. References

[1] Khatib, O., "Real-time Obstacle Avoidance for Manipulators and Mobile Robots," Proceedings of the 1985 IEEE Inter. Conf. on Robotics and Automation, St. Louis, MO, March, 1985.

[2] Sheriden, T.B., "Human Supervisory Control of Robot Systems," Proceedings of the 1986 IEEE Inter. Conf. on Robotics and Automation, San Francisco, CA, April, 1986.

[3] Akin, D.L., Minsky, M.L., Thiel, E.D., and Kurtzman, C.R., "Space Applications of Automation, Robotics and Machine Intelligence Systems (ARAMIS)," MIT report, NASA Contract NAS8-34381, Cambridge, MA, October 1983.

[4] Meintel, A.J., and Schappell, R.T., "Remote Orbital Servicing System Concept," Presented at the Satellite Services Workshop, NASA Johnson Space Center, TX, June 22-24, 1982.

[5] Bronez, M.A., Clarke, M.M., and Quinn, A., " Requirements Development for a Free-Flying Robot - The 'ROBIN'," Proceedings of the 1986 IEEE Inter. Conf. on Robotics and Automation, San Francisco, CA, April, 1986.

[6] Lee, S., Bekey, G., and Bejczy, A.K., "Computer Control of Space-Borne Teleoperators with sensory feedback," Proceedings of the 1985 IEEE Inter. Conf. on Robotics and Automation, St. Louis, MO, April, 1985.

[7] Kohn, W., and Healey, K., "Trajectory Planner for an autonomous free-flying robot," Proceedings of the 1986 IEEE Inter. Conf. on Robotics and Automation, San Francisco, CA, April, 1986.

[8] French, R., Boyce, B., "Satellite Servicing by Teleoperators," Journal of Engineering for Industry, Vol. 107, pp. 49-54, February 1985.

[9] Vafa, Z., "Dynamics of Manipulators in Space", Ph.D. Thesis, Department of Mechanical Engineering, MIT, Cambridge, MA, 1987.

[10] Vafa, Z., and Dubowsky, S., "On the Dynamics of Manipulators in Space Using the Virtual Manipulator Approach," To appear in the Proceedings of the 1987 IEEE Inter. Conf. on Robotics and Automation, Raleigh, NC, March, 1987.

[11] Vafa, Z., Dubowsky, S., "Kinematic and Dynamic Models of Manipulators for use in Space Environments: The Concept of the Virtual Manipulator," To appear in The Proceedings of Seventh World Congress on Theory of Machines and Mechanisms, Sevilla, Spain, 1987.

[12] Yang, D.C.H., Lee, W.L., "Heuristic Combinatorial Optimization in the Design of Manipulator Workspace," IEEE Transactions on Systems, Man, and Cybernetics, Vol. SMC-14, No. 4, July/August 1984.

[13] Kane, T.R., Headrick, M.R., Yatteau, J.D., "Experimental Investigation of an Astronaut Maneuvering Scheme," Journal of Biomechanics, 1972, Vol. 5, pp. 313-320.

Appendix A: Proof of Virtual Manipulator Properties

First it will be proven that for a VM constructed using the rules presented in section 4 of this paper the VM end point will coincide with the end effector. Then it will be proven that when the manipulator goes through a movement the VM joint motions described in section 4 will keep the VM end point on the end effector.

First, recognizing that the system center of mass is stationary in the inertial frame N, $\mathbf{V}_g$ remains stationary in this frame and referring to Figure 2 yields:

$$M_{tot}\mathbf{V}_g = M_N\mathbf{S} + M_{N-1}[\mathbf{S} - \mathbf{L}_{N-1} - \mathbf{T}_{N-1} - \mathbf{R}_{N-1}] + \ldots + M_1[\mathbf{S} - \sum_{i=1}^{N-1}(\mathbf{L}_i + \mathbf{T}_i + \mathbf{R}_i)] \tag{A1}$$

Recall that if the i^{th} joint is revolute $\mathbf{T}_i = 0$, otherwise, its magnitude is equal to the prismatic joint translations from the initial manipulator configuration and its direction is along the translational axis. Equation (A1) can be solved for $\mathbf{S}(t)$ as follows,

$$\mathbf{S}(t) = \mathbf{V}_g + \frac{M_1}{M_{tot}}(\mathbf{R}_1 + \mathbf{T}_1 + \mathbf{L}_1) + \ldots + \frac{M_1 + M_2 + \ldots + M_{N-1}}{M_{tot}}(\mathbf{R}_{N-1} + \mathbf{T}_{N-1} + \mathbf{L}_{N-1}) \tag{A2}$$

Equation (A2) can be written in terms of the vectors $\mathbf{D}_i$, $\mathbf{H}_i$ and $\mathbf{P}_i$ by using Equations (4) through (6), to yield:

$$\mathbf{S}(t) = \mathbf{V}_g + (\mathbf{D}_1 + \mathbf{H}_1 + \mathbf{P}_1) + \ldots + (\mathbf{D}_{N-1} + \mathbf{H}_{N-1} + \mathbf{P}_{N-1}) \tag{A3}$$

Using Equation set (3) and the fact that the end effector position is always equal to $\mathbf{S}(t) + \mathbf{R}_N$ gives:

$$\mathbf{E}(t) = \mathbf{V}_g + \mathbf{V}_1 + \mathbf{P}_1 + \ldots + \mathbf{P}_{N-1} + \mathbf{V}_N \tag{A4}$$

It should be noted that this equation does not depend upon the existance of the Virtual Manipulator. The vector chain represented by Equation (A4) describes the end effector position relative to the N reference frame for all time.

For the initial manipulator position the VM constucted according to the procedure outlined in section 4 has an end point described by the following vector chain,

$$\mathbf{V}_g + \mathbf{V}_1 + \ldots + \mathbf{V}_N \tag{A5}$$

Comparing Equations (A4) and (A5) it follows that in the initial position, when the $\mathbf{P}_i$'s are equal to zero, the end effector coincides with the VM end point.

Now it will be proven that as the real manipulator moves the VM joint motions described in section 4 will keep the VM end point on the real end effector. Say the manipulator goes through some joint movement, from section 4, the following vector chain describes the VM end point, where the $\mathbf{P}_i$'s are no longer zero,

$$\mathbf{V}_g^* + \mathbf{V}_1^* + \mathbf{P}_1^* + \ldots + \mathbf{P}_{N-1}^* + \mathbf{V}_N^* \tag{A6}$$

In the following paragraphs it will be proven that the vectors $\mathbf{V}_i^*$, $\mathbf{V}_g^*$ and $\mathbf{P}_i^*$ in Equation (A6) are the same as $\mathbf{V}_i$, $\mathbf{V}_g$ and $\mathbf{P}_i$ in Equation (A4), respectively, therefore, the VM end point will coincide with the real end effector. The vector $\mathbf{V}_g$ is always constant, therefore,

$$\mathbf{V}_g^* = \mathbf{V}_g \tag{A7}$$

The initial real manipulator links are composed of vectors $\mathbf{L}_{i-1} + \mathbf{R}_i$ and since the manipulator links are rigid, the magnitude of the vectors $\mathbf{L}_{i-1}$ and $\mathbf{R}_i$ and the angles between them are always constant. Since the magnitudes of $\mathbf{L}_{i-1}$ and $\mathbf{R}_i$ are constant, then from Equations (4) and (5) the magnitudes of $\mathbf{H}_{i-1}$ and $\mathbf{D}_i$ will also be constants. It can also be seen that the angles between $\mathbf{H}_{i-1}$ and $\mathbf{D}_i$ are constant. Then

$$|\mathbf{V}_i| = |\mathbf{H}_{i-1} + \mathbf{D}_i| \qquad \forall t, i \tag{A8}$$

The Virtual Manipulator links are composed of the $\mathbf{V}_i^*$ vectors. These links don't change their shapes and lengths as a function of time and since magnitudes of $\mathbf{V}_i^*$ are initially equal to magnitudes of $\mathbf{V}_i$, and magnitudes of $\mathbf{V}_i$ do not change with time it follows that:

$$|\mathbf{V}_i^*| = |\mathbf{H}_{i-1} + \mathbf{D}_i| = |\mathbf{V}_i| \qquad \forall t, i \tag{A9}$$

The magnitude of the vectors $\mathbf{P}_i$ in Equation (A4) and the $\mathbf{P}_i^*$ vectors in Equation (A6) are both obtained from the real manipulator prismatic joint translations, using Equation (6), therefore by definition,

$$|\mathbf{P}_i^*| = |\mathbf{P}_i| \qquad \forall t, i \tag{A10}$$

Now it will be proven that the direction of the vectors $\mathbf{V}_i^*$ and $\mathbf{P}_i^*$ in Equation (A6) are parallel to vectors $\mathbf{V}_i$ and $\mathbf{P}_i$ in Equation (A4), respectively.

First it can be established that the rotations of the first VM link are set equal to the vehicle rotations and hence the first VM link will always be parallel to the vehicle. Therefore,

$$\mathbf{V}_1^* = \mathbf{V}_1 \qquad \forall t \tag{A11}$$

Since axis of rotation or translation of the first real and virtual joints are fixed relative to their corresponding first links, and the rotations of the first VM link is the same as the vehicle, and these axes are initially constructed to be parallel, then they will always be parallel.

Now consider the case when the first real manipulator joint is revolute. The elements of the second VM link $\mathbf{H}_1^*$ and $\mathbf{D}_2^*$ will be parallel to $\mathbf{L}_1$ and $\mathbf{R}_2$ and in turn the vectors $\mathbf{V}_2^*$ and $\mathbf{V}_2$ will be parallel and

$$\mathbf{V}_2^* = \mathbf{V}_2 \qquad \forall t \tag{A12}$$

because the rotational axis of the first VM and real manipulator joints are parallel, as shown above, and the magnitude of their rotations are equal by construction.

In the cases where the first joint is prismatic, the elements of the second VM link $\mathbf{H}_1^*$ and $\mathbf{D}_2^*$ will be parallel to $\mathbf{L}_1$ and $\mathbf{R}_2$ and in turn the vectors $\mathbf{V}_2^*$ and $\mathbf{V}_2$ will be parallel and

$$\mathbf{V}_2^* = \mathbf{V}_2 \qquad \forall t \tag{A13}$$

because the VM and real manipulator translational axis for this joint are parallel. In the same manner it is possible to show that

$$\mathbf{V}_i^* = \mathbf{V}_i \qquad \forall t, i \tag{A14}$$

Also, in a similar manner all the translational axis of the real manipulator and the VM are always parallel, and from Equation (A11),

$$\mathbf{P}_i^* = \mathbf{P}_i \qquad \forall t, i \tag{A15}$$

Substituting Equations (A15), (A14) and (A7) into (A6), and comparing the result with Equation (A4) shows that the end effector will always coincide with the VM end point, and this completes the proof.